Article

Signal-off Electrochemiluminescence Biosensor Based on Phi29 DNA Polymerase Mediated Strand Displacement Amplification For MicroRNA Detection

Anyi Chen, Guofeng Gui, Ying Zhuo, Yaqin Chai, Yun Xiang, and Ruo Yuan

Anal. Chem., **Just Accepted Manuscript** • DOI: 10.1021/acs.analchem.5b01168 • Publication Date (Web): 14 May 2015

Signal-off Electrochemiluminescence Biosensor Based on Phi29 DNA Polymerase Mediated Strand Displacement Amplification For MicroRNA Detection

Anyi Chen, Guo-Feng Gui, Ying Zhuo*, Ya-Qin Chai, Yun Xiang, Ruo Yuan*

Key Laboratory of Luminescent and Real-Time Analytical Chemistry (Southwest University), Ministry of Education, College of Chemistry and Chemical Engineering, Southwest University, Chongqing 400715, China

* Corresponding authors at: Tel.: +86 23 68252277, fax: +86 23 68253172.
E-mail addresses: yingzhuo@swu.edu.cn (Y. Zhuo), yuanruo@swu.edu.cn (R. Yuan).

ABSTRACT

A target induced cycling strand displacement amplification (SDA) mediated by phi29 DNA polymerase (phi29) was firstly investigated and applied in signal-off electrochemiluminescence (ECL) biosensor for microRNA (miRNA) detection. Herein, the target miRNA triggered the phi29-mediated SDA which could produce amounts of single-stranded DNA (assistant probe) with accurate and comprehensive nucleotide sequence. Then, the assistant probe hybridized with the capture probe and the ferrocene-labeled probe (Fc-probe) to form a ternary "Y" structure for ECL signal quenching by ferrocene. Therefore, the ECL intensity would decrease with increasing concentration of the target miRNA, and the sensitivity of biosensor would be promoted on account of the efficient signal amplification of the target induced cycling reaction. Besides, a self-enhanced Ru(II) ECL system was designed to obtain a stable and strong initial signal to further improved the sensitivity. The ECL assay for miRNA-21 detection is developed with excellent sensitivity of a concentration variation from 10 aM to 1.0 pM and limit of detection down to 3.3 aM.

KEYWORDS: electrochemiluminescence, strand displacement amplification, phi29 DNA polymerase, self-enhanced ruthenium composite, microRNA.

INTRODUCTION

MicroRNAs (miRNAs) are a series of short (about 22 nucleotides), endogenous, noncoding ribonucleic acid molecule that have been demonstrated to be promising biomarkers for classification, diagnosis and prognosis of disease, which attract much attention to develop techniques for the detection. [1, 2, 3, 4] In consequence of the intrinsic characteristics of miRNAs, such as short size, sequence similarity among family members, low abundance and susceptibility to degradation, detection techniques with ultrahigh specificity and sensitivity are intensely demanded. Electrochemiluminescence (ECL) detection methodology is promising to meet the needs because of its wide detection range, controlled reaction system, short time consumption, and high sensitivity and signal-to-noise ratio [5, 6]. To realize ECL detection of miRNA, Liao and co-workers have developed an ECL biosensor based on target-triggered circulatory interactions of two hairpin probes and achieved a sensitivity of 10 fM[7]. Cheng's group constructed a distance-dependent ECL resonance energy transfer (ERET) system and developed a biosensor for direct detection with a limit of detection of 21.7 fM[8]. Recently, nucleic acid amplification strategies, such as rolling circle amplification (RCA) [9, 10], loop-mediated isothermal amplification (LAMP) [11] and strand displacement amplification (SDA), have played an important role in the analysis of nucleic acids. On account of the advantages of high efficiency, adaptability, and simple operation, SDA has been widely used in fluorescent assays for the detection of nucleic acid[12, 13]. However, to date, SDA has rarely been applied in ECL assays.

SDA is a nicking endonuclease-assisted isothermal polymerization reaction activated by specific primer and creating products of single-stranded DNA (ssDNA). Commonly, the polymerase used in SDA is Bst 2.0 DNA polymerase[14, 15] or Klenow fragment (exo^-) [16, 17, 18]. However, Bst 2.0 DNA polymerase requires high temperature of 60-72 °C for optimum enzymatic activity and Klenow fragment (exo^-) lacks the ability of continuous polymerization. As a result, the amplification products with Bst 2.0 DNA polymerase or Klenow fragment (exo^-) might contain a large amount of by-products of the non-target DNA fragments, which would decrease the efficiency of the amplification. Recently, we noticed that phi29 DNA polymerase (phi29) has the abilities of extreme strand displacement and high fidelity continuous polymerization at the temperature between 30 °C to 40 °C [19]. Therefore, phi29 has the potential to carry out an SDA reaction with more accurate and comprehensive products, [20] which is promising to improve the sensitivity of detection. As far as we know, phi29-mediated SDA has not been used for miRNA detection before. Thus it was chosen in this work to improve the efficiency of the SDA for signal amplification.

It is well known that a high initial ECL signal is beneficial to improve the sensitivity in a typical signal-off biosensor. [21] Tripropylamine (TPrA), which is easy to oxidized to $TPrA^{\bullet}$ at electrode surface due to its structure of tertiary amidogen, is commonly used as efficient co-reactant to amplify the ECL signal of ruthenium(II) tris(2,2′-bipyridyl) ($Ru(bpy)_3^{2+}$) as $TPrA^{\bullet}$ can promote the creating of excited $Ru(bpy)_3^{2+*}$. [21] Recently, we prepared self-enhanced ECL complexes containing luminous group and co-reactant group in one molecule, which had markedly

promoted the luminous efficiency by reducing energy consumption of co-reaction through intramolecular interaction.[22, 23, 24] Thus, self-enhanced ECL complexes might provide stronger initial signal than directly adding co-reactant into the detection solution. Herein, for the first time, we choose tris(2-aminoethyl)amine (TAEA) as the co-reactant because it has not only the tertiary amidogen, which is similar to TPrA, but also three amino-groups, which can act as crosslinking reagent via the amidations. Therefore, a functionalized self-enhanced Ru(II) complex was prepared by linking TAEA with ruthenium(II) tris(4,4'-dicarboxylicacid-2,2'-bipyridyl) ($Ru(dcbpy)_3^{2+}$) and perylene-3,4,9,10-tetracarboxylic acid (PTCA) through amide bonds respectively. As a result, strong ECL signal can be achieved due to the intramolecular interaction of $Ru(dcbpy)_3^{2+}$ and TAEA. Besides, the luminophore could be stably immobilized on graphene oxide (GO) as PTCA has planiform structure of π-electron delocalization[25, 26, 27], which ensures the stability of the biosensor.

In this work, we report a signal-off ECL biosensor for miRNA detection based on a target induced cycling SDA mediated by phi29. Firstly, a novel self-enhanced ECL luminophore (Scheme 1C), which contains the luminous group of $Ru(dcbpy)_3^{2+}$ and co-reactive group of TAEA in one molecule, is prepared to provide a high initial ECL signal. Then target miRNA (miR-21 is chosen as a model) triggers polymerization reaction from the 3′-end to synthesize a double-stranded DNA based on the template in the presence of phi29 and deoxyribonucleoside triphosphates (dNTPs). Meanwhile, the recognition site for the nicking endonuclease (Nt.BsmAI) is produced, which induces Nt.BsmAI to cleave one strand nick of DNA on a double-stranded DNA

substrate. The following strand displacement synthesis extends the 3'-end at the nick and displaces the downstream DNA strand (assistant probe). Subsequently, a cycling reaction of polymerization and cleaving will continuously produce amounts of assistant probe. In the presence of assistant probe, which has a quantitative relation with the target miRNA, the capture probe hybridizes with ferrocene-labeled DNA (Fc-probe) to form a ternary "Y" junction structure. With the "Y" junction structure building, the initial ECL intensity was quenched by the ferrocene labels through electron transfer and radical reactions. Thus, the quantitative detection of target miRNA can be realized through the decrease of ECL signal to the concentration of target miRNA. Due to the dual signal amplification of phi29-mediated target induced cycling SDA and TAEA-based self-enhanced ECL system, this ECL biosensor achieved ultrasensitive response to the target miRNA.

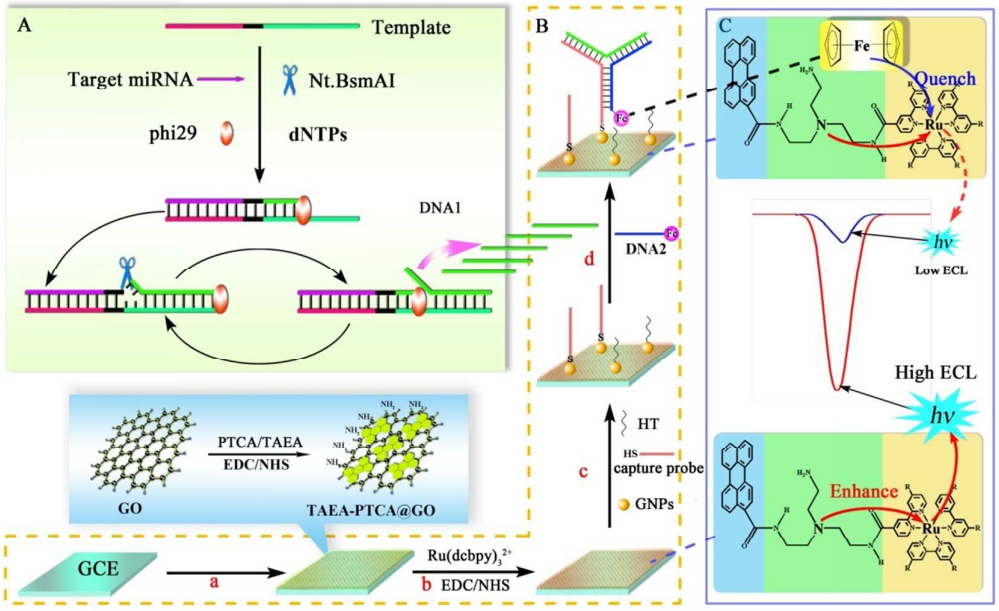

Scheme 1 Schematic diagrams of the sensor: (A) the target induced cycling reaction

based on the phi29-mediated SDA; (B) fabrication of the biosensor: (a) modifying GCE with TAEA-PTCA@GO composite, (b) crosslinking $Ru(dcbpy)_3^{2+}$, (c) assembly of GNPs, capture probe and HT, (d) the forming of "Y" structure; (C) the ECL enhancement mechanism of the self-enhanced Ru(II) composite and the ECL quenching by ferrocene along with the forming of "Y" structure.

EXPERIMENTAL METHODS

Materials and reagents. HPLC-purified microRNA was obtained from Takara Biotechnology Company Ltd. (Dalian, China). The DNA probes were synthesized by Sangon, Inc. (Shanghai, China). The nucleotide sequences are listed in Table 1. The RNase inhibitor diethyl pyrocarbonate (DEPC) was purchase from Sangon, Inc. (Shanghai, China). Phi29 DNA polymerase was purchased from Thermo Fisher Scientific, Inc. (Waltham, MA, USA). Nt.BsmAI was purchased from New England Biolabs, Inc. (Beverly, MA, USA). To create and maintain an RNase-free environment, the solutions were prepared with DEPC-treated water. The tips and tubes were RNase-free and did not require pretreatment to inactivate RNases. Perylene-3,4,9,10-tetracarboxylic dianhydride (PTCDA) was obtained from Lian Gang Dyestuff Chemical Industry Co. Ltd. (Liaoning, China). Graphene oxide (GO) was purchased from Xianfeng Nano Materials Tech Co. Ltd. (Nanjing, China). Tris(2-aminoethyl)amine was supplied from Tokyo Chemicals Industry Development Co. Ltd. (Tokyo, Japan). Tris(4,4′-dicarboxylicacid-2,2′-bipyridyl)ruthenium(II) dichloride[$Ru(dcbpy)_3Cl_2$] was obtained from SunaTech, Inc. (Suzhou, China). N-hydroxysuccinimide (NHS) and N-(3-dimethylaminopropyl)-N′-ethylcarbodiimide hydrochloride (EDC) were received from Shanghai Medpep Co. Ltd. (Shanghai, China). Hexanethiol (HT) was purchased from Sigma (St. Louis, MO, USA). The ultrapure water used for synthesis of the materials was purified by a water purification system with an electrical resistance of 18.2 MΩ·cm. The colloidal gold nanoparticles (GNPs) were prepared by reducing $HAuCl_4$ with sodium citrate at 100 ºC for half an

hour. The buffers involved in this work were prepared as follows: 1×TE buffer (10 mM Tris-HCl, 1.0 mM ethylenediaminetetraacetic acid (EDTA), pH 8.0) was used for dissolving and storing all oligonucleotides; 5×TBE buffer: 445 mM Tris base, 445 mM boric acid, 10 mM EDTA (pH 8.0); Probe immobilization buffer (IB): 10 mM Tris-HCl, 1.0 mM EDTA, 10 mM TCEP, 0.1 M NaCl (pH 7.4); DNA hybridization buffer (HB): 10 mM Tris-HCl, 1.0 mM EDTA, 1.0 M NaCl (pH 7.0).

Table 1 Sequence information for the nucleic acids used in this study

name	sequences*(5′-3′)
template	ATG AAC AGT ATC GCA CCT CTC ACT GTG GAG ACT CAA CAT CAG TCT GAT AAG CTA
assistant probe	ACA GTG AGA GGT GCG ATA CTG TTC AT
miR-21	UAG CUU AUC AGA CUG AUG UUG A
miR-155	UUA AUG CUA AUC GUG AUA GGG GU
TBA	HS-$(CH_2)_6$-GGT TGG TGT GGT TGG
Apt-PDGF	H_2N-$(CH_2)_6$-TTT TTT TTT TCA GGC TAC GGC ACG TAG AGC ATC ACC ATG ATC CTG
Fc-probe	TGT AAT CGC ATC TTG GAC-Fc
capture probe	HS-AAA TGT CCA AGA CCT CTC ACT GT

Apparatus. The ECL measurements were performed on a model MPI-A electrochemiluminescence analyzer (Xi′An Remax Electronic Science & Technology

Co. Ltd., Xi′An, China) with a conventional three-electrode system used with Ag/AgCl (saturated KCl) as reference electrode, a platinum wire as counter electrode and a modified glass carbon electrode (GCE, Φ=4 mm) as working electrode in the experiment. Electrochemical measurement was carried out with a CHI660C electrochemistry workstation (Shanghai Chenhua Instruments, China) with a three-electrode electrochemical cell consisted of a modified glass carbon electrode (GCE, Φ=4 mm) as working electrode, a platinum wire as counter electrode, and a saturated calomel electrode (SCE) as reference electrode. The surface appearance of grapheme oxide composites were characterized by scanning electron microscopy (SEM, S-4800, Hitachi, Tokyo, Japan) at an acceleration voltage of 30 kV. UV-vis absorption spectra were carried out on UV-2450 UV-vis spectrophotometer (Shimadzu, Tokyo, Japan). Fluorescence spectra of TAEA-PTCA were carried out on RF-5301PC spectrophotometer (Shimadzu, Tokyo, Japan) with a 150W Xenon lamp (Ushio Inc, Japan) as the excitation source at room temperature. Raman spectra of the pure substances and composites were carried out on a Renishaw inVia confocal Raman microscope system (Renishaw, UK).

Preparation of TAEA-PTCA@GO composite. First, PTCDA (1 mg) was dissolved in sodium hydroxide aqueous solution (NaOH, 10 mM, 8 mL), then pale yellow aqueous solution with conspicuous green fluorescence was obtained. Then hydrochloric acid was added into the solution until pH=4, meanwhile, the aqueous solution turned red. After that, 2 mL of solution containing 40 mM EDC and 10 mM NHS was dispersed with this red solution. The mixed solution was stirred at ice point

for 4 hours. Next, 2 mL of solution containing 50 mM TAEA and 1mg GO was added into this mixed solution and stirred at room temperature for 48 hours. In this progress, the mixed solution turned from red to amaranthine. Then sodium hydroxide solution was used to deal with the product followed by centrifuging and rinsing with ultrapure water for three times to remove the upper solution. At last, the precipitate was dissolved in 2 mL of ultrapure water for further use.

Strand displacement amplification. For feasibility investigation, 1 pM primer (miR-21), 1 pM assistant probe and 1pM template were first mixed in reaction buffer (50 mM Tris-acetate, 10 mM Mg-acetate, 66 mM K-acetate, pH 7.5, 25 ℃). Then, the mixture was heated to 95 ℃ for 5 min and slowly cooled down to room temperature in about 4 h to ensure a relatively complete hybridization of the miR-21 with the template. After the addition of 500 μM dNTPs, 100 U/mL Nt.BsmAI and 100 U/mL phi29, the mixture was allowed to react at 37 ℃ for 2 h in a constant temperature incubator. Finally, the reaction system was terminated by a thermal treatment at 65 ℃ for 10 min, and the resulted products were stored at 4 ℃. In sensitivity investigation experiments, targets with different concentrations were annealed with 1 pM assistant probe and 1 pM template, and other operations were as fore-mentioned.

Non-denaturing polyacrylamide gel electrophoresis (PAGE). To carry out PAGE, four samples were prepared of 2 μM assistant probe, a mixture of miR-21 and template (1 μM miR-21 and 1 μM template included), amplification product by SDA (1 μM miR-21 and 1 μM template used), and a mixture of 2 μM capture probe, 2 μM assistant probe and 2 μM Fc-probe, respectively. The samples were loaded into the

notches of the freshly prepared polyacrylamide gel (16%), and electrophoresis was performed at 100 V for 60 min in 1×TBE buffer. After dying with ethidium bromide (EB), the gel was removed to a dark box. Then the electrophoresis image of the polyacrylamide gel was taken by using a digital camera under UV light.

Fabrication of the self-enhanced ECL biosensor. The glassy carbon electrode (GCE, Φ=4 mm) was firstly polished on a polishing cloth with 0.3 and 0.05 μm alumina powder respectively to obtain a mirror-like surface, and was sonicated with ethanol and ultrapure water. The sol of TAEA-PTCA@GO composite was simply prepared by separating the composite into 1mL of ultrapure water. Then, 8 μL of the sol was dropped on the polished glassy carbon electrode and dried at room temperature. The TAEA-PTCA@GO composite on the GCE would turn into stable film which could be used as the substrate of the ECL biosensor. Next, EDC/NHS activated $Ru(dcbpy)_3Cl_2$ (10 mM) aqueous solution was dropped on the TAEA-PTCA@GO composite base and incubated for 12 h at room temperature. After rinsed and dried, the colloidal GNPs were absorbed on the composite taking advantage of the coulomb force between the amidogen. Then the capture probe (1 μM, IB) was fabricated on the surface of the electrode. Finally, 10 μL of HT (1.0 mM, ethanol) was drop-coated onto the modified electrode surface and incubated for 30 min to block the nonspecific binding sites.

Measurement procedure. To measure the ECL signal, 5 μL products of SDA as well as 5 μL of Fc-probe (1 μM, HB) should be dropped onto the surface of the biosensor and incubated at room temperature for 30 min. After incubation, the

biosensor was rinsed with ultrapure water remove the unbound reagents. With the modified GCE as the working electrode, Ag/AgCl (saturated KCl) as the reference electrode and a platinum wire as auxiliary electrode, a conventional three-electrode system was constructed to carry out ECL measurement. CV mode, which with a continuous potential scanning from 0.2 to 1.2 V at a scanning rate of 100 mV/ s, was applied to achieve ECL spectra in PBS (pH 7.4).

RESULTS AND DISCUSSION

Investigation of the proposed phi29-mediated SDA. The performance of this SDA is verified by native polyacrylamide gel electrophoresis (PAGE). As shown in Figure 1, the stator (assistant probe) in lane 1 exhibits a distinct single band. Lane 2 shows the PAGE result for the amplification product by SDA in the absence of phi29 and Nt.BsmAI, exhibiting distinct single band, indicating that no reaction occurs. The bright band could be attributed to the hybridization of miR-21 and the template. When the reaction is conducted in the presence of phi29 and Nt.BsmAI, the dual-band, consisting of a band matching the assistant probe and another band matching the hybridization of miR-21 and the template, shows that there is assistant probe produced in the reaction (lane 3 in Figure 1). The narrow band matching the assistant probe means very homogeneous amplification products of this reaction. The single band in lane 4 demonstrates that the “Y” structure is formed successfully.

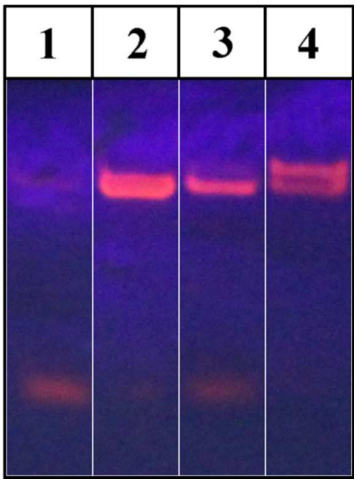

Figure 1 PAGE analysis of different samples. Lane 1: 2 μM assistant probe; lane 2: a mixture of miR-21 and template (1 μM miR-21 and 1 μM template included); lane 3: amplification product by SDA (1 μM miR-21 and 1 μM template included); lane 4: a mixture of 2 μM capture probe, 2 μM assistant probe and 2 μM Fc-probe. Solutions were heated to 95 °C for 5 min and then slowly cooled to room temperature for at least 1 h.

Characterization of different materials. Scanning electron microscope (SEM) is employed to characterize the surface morphology of GO and TAEA-PTCA@GO composite. Figure 2A shows the SEM image of GO, which has a paper-like morphology and is easy to be folded. TAEA-PTCA@GO composite has a thicker board-like morphology rather than paper-like morphology of GO as Figure 2B shows, which indicates that TAEA-PTCA complex has been stacked on GO uniformly.

To characterize the structure of TAEA-PTCA, UV-vis absorption spectra are measured. In ethanol solution, the absorption bands of PTCA appear in the region of 400-500 nm (Figure 2C curve a), while that of TAEA-PTCA complex appear in the

region of 450-550 nm (Figure 2C curve b). This red shift could be attributed to the inductive effect of TAEA, which indicates the covalent linking of TAEA and PTCA. Furthermore, in aqueous solution (Figure 2C curve c), the absorption bands of TAEA-PTCA complex appear in the region of 450-550 nm, which is identical with the situation in ethanol solution. Nevertheless, in equal concentration, the characteristic of the absorption bands in aqueous solution is quite different from that in ethanol solution and the absorbance is much lower. The differences of the spectra in different solvents are attributed to strong hydration and ionization of TAEA-PTCA complex in aqueous solution, which indicates the existence of amine groups in TAEA-PTCA complex.

Raman spectra are employed to characterize the assembly of TAEA-PTCA@GO composite. As show in Figure 2D curve a, in the case of 532 nm excitation, the Raman spectrum of GO displays two remarkable peaks at about 1350 and 1600 cm^{-1}, which corresponds to the typical D-band and G-band. However, in the Raman spectrum of TAEA-PTCA@GO (Figure 2D curve b), these signals are superimposed by the TAEA-PTCA spectrum presenting features at 1250 cm^{-1} (N-H bending of Amide III), 1299 and 1377 cm^{-1} (in-plane ring "breathing"), 1456 cm^{-1} (ring deformation), 1571 cm^{-1} (in-plane C–C stretching), and 1696 cm^{-1} (imide bending). When covered with TAEA-PTCA, the D-band is not as clear as the common GO since D-band demonstrates the flaw of graphene materials. TAEA-PTCA exhibits observable fluorescence when being resonantly excited in the region between 450 nm and 600 nm (see Figure S1, SI), however, no obvious emission background is present

in the Raman spectrum of TAEA-PTCA@GO composite, indicating pronounced quenching because of the electronic communication with GO.

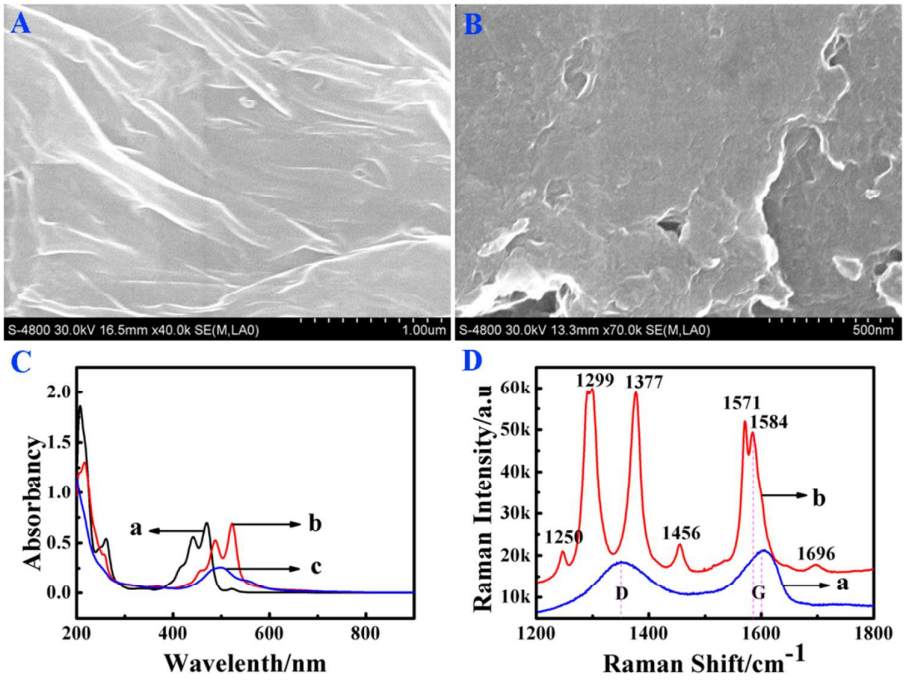

Figure 2 SEM images of GO (A) and TAEA-PTCA@GO (B); (C) UV-vis absorption spectra of PTCA in ethanol (a), TAEA-PTCA in ethanol (b) and TAEA-PTCA in water (c); (D) Raman spectra of GO (a) and TAEA-PTCA@GO (b). Raman spectra were recorded with a laser excitation wavelength of 532 nm.

Electrochemical Behaviors of the biosensor. To confirm the process of the ECL sensor fabrication, we employed the cyclic voltammograms (CVs) experiments to characterize different assembled electrodes in 5.0 mM $[Fe(CN)_6]^{3-/4-}$ solution. As shown in Figure 3A, a pair of the apparent redox peaks of $[Fe(CN)_6]^{3-/4-}$ can be observed on the bare GCE (curve a). After modifying with TAEA-PTCA@GO composite on the bare GCE surface, an obvious decrease in redox current was observed (curve b). When $Ru(dcbpy)_3^{2+}$ was cross-linked on the surface of

TAEA-PTCA@GO composite, the CV curve shifted to positive direction integrally (curve c). Then gold nanoparticles (GNPs) were dropped on the electrode, the redox peak current was enhanced, suggesting that GNPs brought excellent conductivity and large surface area to promote the electron transfer (curve d). When the thiol-modified capture probe (CP) was fabricated on the electrode with the help of GNPs, the redox current was decreased (curve e). After using HT to block the nonspecific binding sites, the redox current was decreased further (curve f). As expected, when the modified electrode was incubated with the assistant probe and the Fc-probe, the current responses declined (curve g). Such results could be attributed to the inhibition of "Y" structure to the electron transfer.

Detection of miR-21 with the biosensor. The performance of the proposed biosensor is monitored by incubating with product of SDA and Fc-probe. The ECL intensity of the biosensor decreases with increasing concentration of miR-21. The calibration plot shows a good linear relationship between ECL responses and the logarithmic value of miR-21 concentrations ranging from 10 aM to 1 pM with a correlation coefficient of 0.996 (Figure 3B). The regression equation is I = -14114.77-1281.74lg(c/M) (where I stands for the ECL intensity and c stands for the concentration of miR-21) with a detection limit of 3.3 aM. With the calibration of ECL curve, a wide dynamic concentration response range of 10 aM - 1 pM is obtained. This signal-off biosensor provides an easier and more effective way as well as a wider dynamic concentration response range to quantify miR-21.

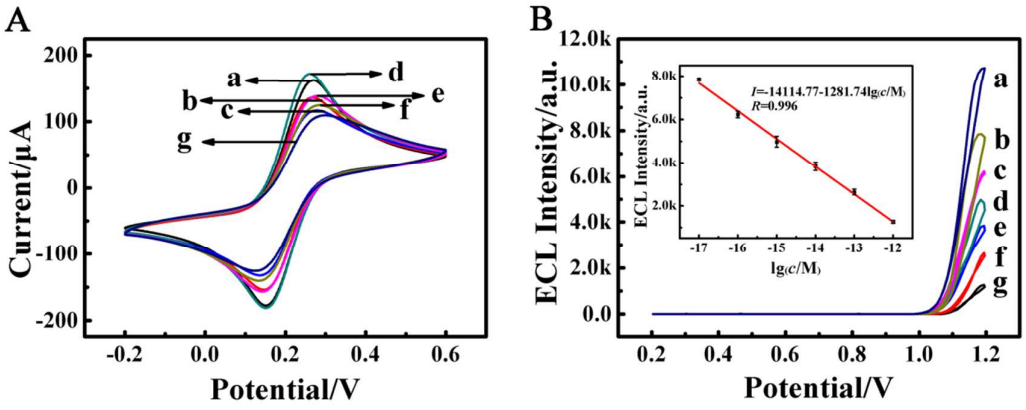

Figure 3 (A) CVs at the (a) bare GCE, (b) TAEA-PTCA@GO/GCE, (c) Ru-TAEA-PTCA@GO/GCE, (d) GNPs/Ru-TAEA-PTCA@GO/GCE, (e) CP/GNPs/Ru-TAEA-PTCA@GO/GCE, (f) HT/Probe/GNPs/Ru-TAEA-PTCA@GO/GCE, (g) assistant probe and Fc-probe/HT/CP/GNPs/Ru-TAEA-PTCA @GO/GCE in 5.0 mM $[Fe(CN)_6]^{3-/4-}$ by scanning the potential from -0.2 to 0.6 V (vs SCE) at a scan rate of 0.05 V/s. (B) ECL profiles of the biosensor for miRNA detection at different concentrations: (a) blank, (b) 0.01 fM, (c) 0.1 fM, (d) 1 fM, (e) 0.01 pM, (f) 0.1 pM and (g) 1 pM. The insert was calibration curve for miRNA determination. All ECL signals were measured in 0.1 M PBS (pH 7.4) by scanning the potential from 0.2 to 1.2 V (vs Ag/AgCl) at a scanning rate of 100 mV/ s.

Table 2 The Comparison for Existing miRNA Detection Methods

methods	detection limit	dynamic rang	reference
ECL	10 fM	10 fM ~1 pM	7
Fluorescent	1 fM	1 fM ~10 nM	12
Electrochemical	1 fM	1 fM ~10 pM	28
ECL	1fM	1 fM ~1 pM	29
Fluorescent	10 fM (37 °C) 1 aM (4 °C)	10 fM ~1 nM 1 aM ~10 fM	14
Electrochemical	5 aM	10 aM ~10 fM	30
ECL	3.3 aM	10 aM ~1 pM	this work

Selectivity of the biosensor. To evaluate the selectivity and specificity of the present biosensor, other ssDNAs or RNAs are employed as interfering substances, such as miR-155, thrombin aptamer (TBA), and platelet derived growth factor-binding aptamer (Apt-PDGF). As shown in Figure 4A, the contrast experiments were performed by using miR-155 (1 pM), TBA (1 pM), and Apt-PDGF (1 pM) to replace miR-21 (1 pM) respectively. We can see that the ECL signal of miR-155, TBA, and Apt-PDGF did not exhibit any obvious decrease compared with the blank. The mix containing 1 pM miR-21, 1 pM miR-155, 1 pM TBA, 1 pM Apt-PDGF was tested by the biosensor. When the ECL response of the mixture was compared with

that obtained from the 1 pM miR-21 only, no remarkable difference was found. They all indicated that the ECL intensity in the presence of miR-21 was much weaker than those of the others, which meant that miR-155, TBA, and Apt-PDGF had no obvious influence on the response to miR-21, and indicated that the biosensor displayed good selectivity and specificity for the determination of miR-21.

Stability of the miRNA biosensor. Stability is one of the important factors to judge the performance of the biosensor, especially in signal-off biosensor as the ECL substrate suffers challenges to the property of film-forming and water-tolerant. In order to adequately investigate whether the self-enhanced ECL composite (Ru-TAEA-PTCA@GO) can meet the needs of cyclic potential scan for long testing process, the stability of the proposed biosensor was studied under continuous scanning for 180 seconds in 0.1 M PBS (pH 7.4) (see Figure S2, SI). We also showed the stability of the biosensor with 3 cycles at different concentrations. As we can see from Figure 4B, the results suggested that the stability of the proposed biosensor was good.

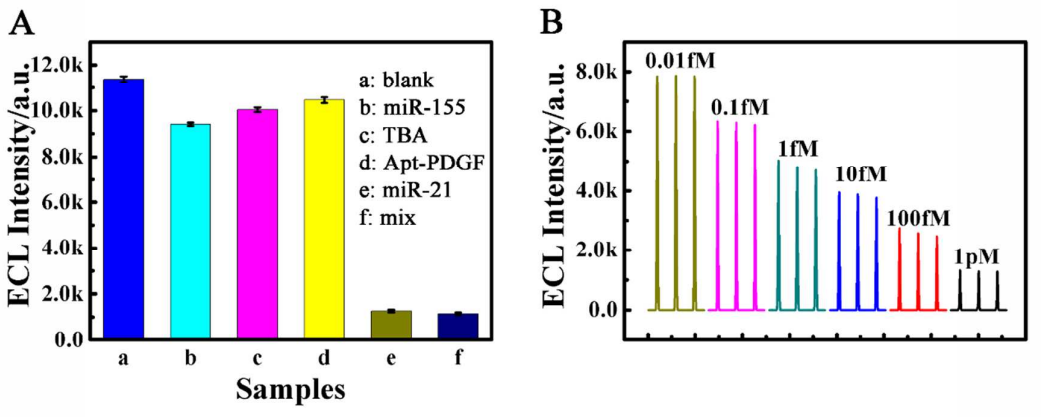

Figure 4 (A) Selectivity investigation for miR-21 (1 pM) detection against the

interference nucleic acids: miR-155 (1 pM), TBA (1 pM), Apt-PDGF (1 pM), Mixture (containing 1 pM miR-21, 1 pM miR-155, 1 pM TBA, 1 pM Apt-PDGF). (B) The ECL stability of proposed biosensor. All ECL signals were measured in 0.1 M PBS (pH 7.4) by scanning the potential from 0.2 to 1.2 V (vs Ag/AgCl) at a scanning rate of 100 mV/ s.

Application of the biosensor in tumor cells. To investigate the capacity of the proposed biosensor for detection of tumor cell extractions, human lung adenocarcinoma cell line (A549) was selected to perform an ECL assay to measure the expression of miR-21. The cell samples were processed by a commercial miRNA extraction kit after cell counting. The sensitivities were explored by setting the cell concentration as 10^1 cells to 10^6 cells (Figure 5, blue x-axis). Through linear regression analysis of sensitivity data, the R value of 0.995 was achieved, which showed a good linear relation. Compared with standard samples (Figure 5, red x-axis), the calibration curve for practical samples demonstrated an approximate slope, which manifested a good adaptability of the biosensor to practical samples.

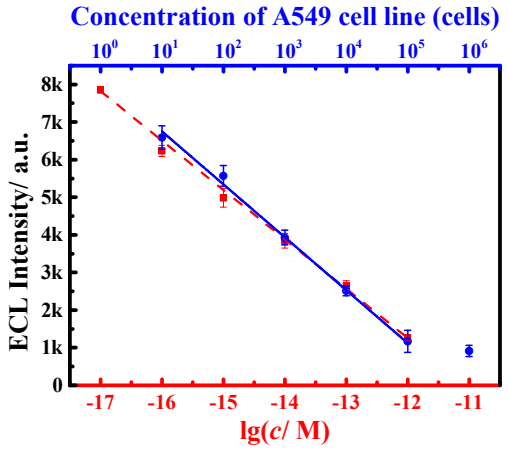

Figure 5 Application of the biosensor in A549 cell line and data analysis.

CONCLUSIONS

In summary, a signal-off ECL biosensor is constructed for highly specific and sensitive detection of miRNA based on a target cycling amplification of a novel phi29-mediated SDA. Significantly, under mild condition (the physiological temperature), the newly designed SDA has achieved homogeneous amplification products and high efficiency. Furthermore, with the help of high initial ECL intensity provided by self-enhanced Ru-TAEA-PTCA@GO composite, the present assays can provide sensitive way as well as a wide dynamic concentration response range for the accurate detection of miRNA. The application in tumor cells indicates that the biosensor could achieve good performance in practical sample analysis. We believe that this proposed biosensor holds great potential for further application in biomedical research and early clinical diagnostics.

ASSOCIATED CONTENT

Supporting Information

The fluorescence spectra and ECL stability under continuous scanning are provided as Supporting Information. This material is available free of charge via the Internet at http://pubs.acs.org.

AUTHOR INFORMATION

*** Corresponding authors**

Tel.: +86 23 68252277, fax: +86 23 68253172.

E-mail addresses: yingzhuo@swu.edu.cn (Y. Zhuo), yuanruo@swu.edu.cn (R. Yuan).

Notes

The authors declare no competing financial interest.

ACKNOWLEDGMENT

This work was financially supported by the NNSF of China (21275119, 51473136), and the Fundamental Research Funds for the Central Universities **(**XDJK2015A002, XDJK2014A012), China.

REFERENCES

(1) Válóczi, A.; Hornyik, C.; Varga, N.; Burgyán, J.; Kauppinen S.; Havelda, Z. *Nucleic Acids Res.* **2004**, 32, e175.

(2) Chen, C.; Ridzon, D. A.; Broomer, A. J.; Zhou, Z.; Lee, D. H.; Nguyen, J. T.; Barbisin, M.; Xu, N. L.; Mahuvakar, V. R.; Andersen, M. R.; Lao, K. Q.; Livak K. J.; Guegler, K. J. *Nucleic Acids Res.* **2005**, 33, e179.

(3) Dong, H. F.; Jin, S.; Ju H. X.; Hao, K. H.; Xu, L. P.; Lu, H. T.; Zhang, X. J. *Anal. Chem.* **2012**, 84, 8670-8674.

(4) Dong, H. F.; Lei, J. P.; Ding, L.; Wen, Y. Q.; Ju, H. X.; Zhang, X. J. *Chem. Rev.* **2013**, 113, 6207-6233.

(5) Richter, M. M. *Chem. Rev.* **2004**, 104, 3003−3036.

(6) Hu, L. Z.; Xu, G. B. *Chem. Soc. Rev.* **2010**, 39, 3275–3304.

(7) Liao, Y. H.; Huang, R.; Ma, Z. K.; Wu, Y. X.; Zhou X. M.; Xing, D. *Anal. Chem.* **2014**, 86, 4596-4604.

(8) Cheng, Y.; Lei, J. P.; Chen Y. L.; Ju, H. X. *Biosens. Bioelectron.* **2014**, 51, 431-436.

(9) Harcourt, E. M.; Kool, E. T. *Nucleic Acids Res.* **2012**, 40, e65.

(10) Hong, C. A.; Jang, B.; Jeong, E. H.; Jeong H.; Lee, H. *Chem. Commun.* **2014**, 50, 13049-13051.

(11) Hsieh, K.; Mage, P. L.; Csordas, A. T.; Eisenstein M.; Soh, H. T. *Chem. Commun.* **2014**, 50, 3747-3749.

(12) Yin, B. C.; Liu, Y. Q.; Ye, B. C. *Anal. Chem.* **2013**, 85, 11487-11493.

(13) Zhang, L. R.; Zhu, G. C.; Zhang, C. Y. *Anal. Chem.* **2014**, 86, 6703-6709.

(14) Duan, R. X.; Zuo, X. L.; Wang, S. T.; Quan, X. Y.; Chen, D. L.; Chen, Z. F.; Jiang, L.; Fan C. H.; Xia, F. *J. Am. Chem. Soc.* **2013**, 135, 4604−4607.

(15) Yu, Y.; Chen, Z. G.; Shi, L. J.; Yang, F.; Pan, J. B.; Zhang B. B.; Sun, D. P. *Anal. Chem.* **2014**, 86, 8200-8205.

(16) Zou, B. J.; Song, Q. X.; Wang, J. P.; Liu, Y. L.; Zhou, G. H. *Chem. Commun.* **2014**, 50, 13722-13724.

(17) Shi, C.; Liu, Q.; Ma, C. P.; Zhong, W. W. *Anal. Chem.* **2014**, 86, 336-339.

(18) Dong, H. F.; Zhang, J.; Ju, H. X.; Lu H. T., Wang, S. Y.; Jin, S.; Hao, K. H.; Du, H. W.; Zhang, X. J. *Anal. Chem.* **2012**, 84, 4587-4593.

(19) Alsmadi, O.; Alkayal, F.; Monies D.; Meyer, B. F. *BMC Res. Notes.* **2009**, 2, 48.

(20) Paez, J. G.; Lin, M.; Beroukhim, R.; Lee, J. C.; Zhao, X. J.; Richter, D. J.; Gabriel, S.; Herman, P.; Sasaki, H.; Altshuler, D.; Li, C.; Meyerson, M.; Sellers, W. R.; *Nucleic Acids Res.* **2004**, 32, e71.

(21) Cao, W.; Ferrance, J. P.; Demas, J.; Landers, J. P.; *J. Am. Chem. Soc.* **2006**, 128, 23, 7572-7578.

(22) Zhuo, Y.; Liao, N.; Chai, Y. Q.; Gui, G. F.; Zhao, M.; Han, J.; Xiang, Y.; Yuan, R. *Anal. Chem.* **2014**, 86, 1053-1060.

(23) Wang, H. J.; He, Y.; Chai, Y. Q.; Yuan, R. *Nanoscale* **2014**, 6, 10316–10322.

(24) Gui, G. F.; Zhuo, Y.; Chai, Y. Q.; Xiang Y.; Yuan, R. *Anal. Chem.* **2014**, 86, 5873-5880.

(25) Wang, Q. H.; Hersam, M. C. *Nat. Chem.* **2009**, 1, 206-211.

(26) MacLeod, J. M.; Rosei, F.; *small* **2014**, 10, 1038-1049.

(27) Kozhemyakina, N. V.; Englert, J. M.; Yang, G.; Spiecker, E.; Schmidt, C. D.; Hauke F.; Hirsch, A. *Adv. Mater.* **2010**, 22, 5483-5487.

(28) Lin, M. H.; Wen, Y. L.; Li, L. Y.; Pei, H.; Liu, G.; Song, H. Y.; Zuo, X. L.; Fan, C. H.; Huang, Q. *Anal. Chem.* **2014**, 86, 2285-2288.

(29) Liu, W. P.; Zhou, X. M.; Xing, D.; *Biosens. Bioelectron.* **2014**, 58. 388-394.

(30) Labib, M.; Khan, N.; Ghobadloo, S. M.; Cheng, J.; Pezacki, J. P.; Berezovski M. V. *J. Am. Chem. Soc.* **2013**, 135, 3027-3038.

For TOC only

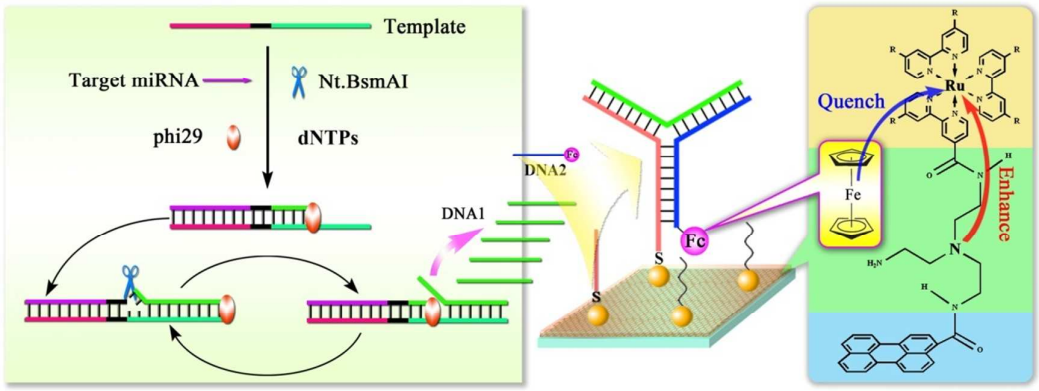
Template
Target miRNA
Nt.BsmAI
phi29
dNTPs
DNA1
DNA2
Fc
S
S
Quench
Ru
Fe
Enhance
N